International Journal of Pharmaceutics, 51 (1989) 147–156
Elsevier

IJP 01726

Determination of crystal growth kinetics from desupersaturation measurements

G.L. Zipp and N. Rodriguez-Hornedo

College of Pharmacy, University of Arizona, Tucson, AZ 85721 (U.S.A.)

(Received 9 June 1988)
(Modified version received 19 September 1988)
(Accepted 23 September 1988)

Key words: Crystallization; Precipitation; Growth rate; Oxalic acid dihydrate

Summary

The growth kinetics of oxalic acid dihydrate have been determined in a multiparticle suspension by measuring (a) the solution concentration during growth and (b) the final crystal size distribution. The method of calculation involves the use of the number mean size together with the second and third moments of the product size distribution. It is necessary to assume that the number of crystals remains constant and that crystal growth rate is independent of size.

Introduction

The ability to predict and modify the final crystal size distribution of a drug is an important step in the design and development of many pharmaceuticals. For instance, one of the methods used to prepare parenteral suspensions is the combination of two sterile solutions. The crystals are formed in situ and further size classification is not desirable (or possible).

The crystal size distribution (CSD) affects such properties as dissolution rate, filtration rate, compression characteristics and fluidization factors. The CSD from a crystallizer can be modified by altering operating conditions, solvent systems or through selective size destruction techniques. Through the use of a model describing the crystallization process different systems can be tested and operational conditions optimized before implementation in production.

Essential requirements for any crystallization model are values of the growth and nucleation kinetics of the system. Presented here is a method of evaluating the growth rate of a substance as a function of supersaturation. A crystallization experiment, where the desupersaturation profile is monitored as a function of time and the final CSD is measured, would provide the necessary data to calculate the growth rate kinetics.

Rodriguez-Hornedo and Carstensen (1986), and Rodriguez-Hornedo (1984) developed a model that describes the non-isothermal crystallization of oxalic acid dihydrate. Experimentally measured desupersaturation profiles were used in conjunction with previously reported values of the growth and nucleation exponents of oxalic acid dihydrate to predict the product size distribution from the crystallizer.

In the method of analysis presented here the procedure recommended by De Silva et al. (1980)

Correspondence: N. Rodriguez-Hornedo, Department of Pharmaceutical Sciences, College of Pharmacy, University of Arizona, Tucson, AZ 85721 U.S.A.

is used to calculate growth rate kinetics of oxalic acid dihydrate from aqueous solution. This method requires less computational effort and is based on a more elegant theoretical basis than the method developed by Rodriguez-Hornedo and Carstensen. It uses the final product size distribution and the desupersaturation profile to back-calculate the rate at which the crystals grew rather than varying model parameters until the correct results are obtained. The model of De Silva et al. does not put any constraints on the CSD of the product and does not require previous knowledge of the growth and nucleation exponents.

The ease of application of this method to the typical experimental data of a pharmaceutical crystallization experiment makes it ideal for evaluation of crystal growth rates.

Theory

The rate at which the crystals grow is defined as the change in linear size per unit time. This is usually expressed as:

$$G = \frac{dL}{dt} \tag{1}$$

where G is the linear growth rate, L is the crystal length and t is time. Misra and White (1973) show how the growth rate of crystals can be determined in a batch crystallizer by measuring changes in the cumulative number distribution with time. However, sampling of intermediate crystal size distributions can be difficult. Thus, it is convenient to be able to calculate growth rates knowing only the final crystal size distribution and solution concentration as a function of time during the crystallization process.

The amount of crystal mass formed, dM, in a time period, dt, is equivalent to the change in concentration, dC, during the same period. A mass growth rate can now be defined as:

$$\frac{dM}{dt} = \frac{-dC}{dt} \tag{2}$$

where M is the crystalline mass (g/g-solvent), C is the solution concentration (g/g-solvent) and t is time (min). In the case of seeded crystallization, where the seeds are monodisperse and if nucleation is negligible, the change in crystal mass can be related to the growth rate as:

$$\frac{dM}{dt} = \frac{d}{dt}\left(\rho k_v N_t L^3\right) = 3\rho k_v N_t L^2 \frac{dL}{dt} \tag{3}$$

where ρ is the crystal density, k_v is the volume shape factor, and N_t is the number of crystals per gram of solvent. Because the rate of mass depletion from the solution is affected by the crystal surface area, the growth rate is normalized for the surface area of the crystals, A. Dividing by the total crystal area, we obtain:

$$\frac{1}{A}\frac{dM}{dt} = \frac{\left(3\rho k_v N_t L^2\right)}{N_t k_a L^2}\frac{dL}{dt} \tag{4}$$

where k_a is the surface shape factor. The linear growth rate, G, can be evaluated from the rate of mass depletion from the solution in Eqn. 4 as:

$$\frac{dL}{dt} = \frac{k_a}{3\rho k_v}\frac{1}{A}\frac{dM}{dt} \tag{5}$$

If the seed crystals are assumed to be spherical in shape, Eqn. 5 can be simplified. The volume of a spherical crystal is $V_{\text{sphere}} = (\pi/6)L^3$ and the area is $A_{\text{sphere}} = \pi L^2$ from which k_v is $\pi/6$ and k_a is π. Thus, the ratio of surface shape factor to volume shape factor is 6 and Eqn. 5 becomes:

$$G = \frac{dL}{dt} = \frac{2}{\rho A}\frac{dM}{dt} \tag{6}$$

Crystal growth rate is often expressed as a function of supersaturation and temperature by the following empirical relationship:

$$G = k_g \sigma^a \tag{7a}$$

or

$$G = k'_g s^a \tag{7b}$$

An explanation of symbols is included in the Nomenclature.

From Eqns. 7a or 7b it can be seen that the dependence of growth rate on supersaturation can be determined in a crystallization experiment conducted at constant temperature. If the growth rate is measured in a series of concentrations, a plot of $\ln G$ vs. $\ln s$ will yield the values of $\ln k_g'$ and a as the intercept and slope of a straight line through the points. Likewise, $\ln k_g$ and a can be found from a plot of the $\ln G$ vs $\ln \sigma$.

Since the seed crystals are not monodisperse, and not guaranteed to be spherical in shape, there will be an entire size range of crystals with shape and area factors different from spheres. To account for this, the population balance approach can be used to develop a more general analysis.

Randolph and Larson (1973) define population density to be the number of crystals in a size range. That is,

$$n = \frac{\mathrm{d}N}{\mathrm{d}L} \tag{8}$$

where n is the population density (no./μg-solvent) and $\mathrm{d}N$ is the number of crystals per gram of solvent, (no./g-solvent), in the size range $\mathrm{d}L$ (μm).

The moments of the distribution are defined as

$$m_j = \int_0^\infty L^j n \, \mathrm{d}L \tag{9}$$

where m_j is the j^{th} moment of the distribution. They are used to describe statistical parameters of the distribution. For example, the average size of the crystals, $\bar{L}$, is the total length of crystals, m_1, divided by the total number of crystals, m_0,

$$\bar{L} = \frac{\int_0^\infty L n \, \mathrm{d}L}{\int_0^\infty n \, \mathrm{d}L} = \frac{m_1}{m_0} \tag{10}$$

Likewise, the variance about the mean, μ_2, and the skew, μ_3, can be expressed in terms of the moments as:

$$\mu_2 = \frac{\int_0^\infty (L-\bar{L})^2 n \, \mathrm{d}L}{\int_0^\infty n \, \mathrm{d}L} = \frac{m_2}{m_0} - \frac{m_1^2}{m_0^2} = \frac{m_2}{m_0} - \bar{L}^2 \tag{11}$$

$$\mu_3 = \frac{\int_0^\infty (L-\bar{L})^3 n \, \mathrm{d}L}{\int_0^\infty n \, \mathrm{d}L}$$

$$= \frac{m_3}{m_0} - \frac{3m_1m_2}{m_0^2} + \frac{2m_1^3}{m_0^3}$$

$$= \frac{m_3}{m_0} - 3\frac{m_2}{m_0}\bar{L} + 2\bar{L}^3 \tag{12}$$

The total crystal surface area, A, and the total mass of crystals, M, can be expressed in terms of the moments as

$$A = k_a \int_0^\infty L^2 n \, \mathrm{d}L = k_a m_2 \tag{13}$$

$$M = \rho k_v \int_0^\infty L^3 n \, \mathrm{d}L = \rho k_v m_3 \tag{14}$$

From Eqns. 11 and 13

$$A = k_a m_2 = \left(\mu_2 + \bar{L}^2\right) k_a m_0 \tag{15}$$

and from Eqns. 12 and 14

$$M = \rho k_v m_3 = \left(\mu_3 + 3\bar{L}\mu_2 + \bar{L}^3\right) \rho k_v m_0 \tag{16}$$

By substituting Eqns. 15 and 16 into Eqn. 5, we obtain an expression for the growth rate:

$$\frac{\mathrm{d}L}{\mathrm{d}t} = \frac{1}{3\left(\mu_2 + \bar{L}^2\right)} \frac{\mathrm{d}}{\mathrm{d}t}\left(\mu_3 + 3\bar{L}\mu_2 + \bar{L}^3\right) \tag{17}$$

If the crystal growth rate is not a function of crystal size, and nucleation or crystal breakage do not occur, the shape of the CSD will not change. As the crystals grow the distribution will shift to larger sizes but the values of μ_2 and μ_3 will be constant. Then, taking the derivative on the right hand side of Eqn. 17 one obtains

$$\frac{\mathrm{d}L}{\mathrm{d}t} = \frac{\mathrm{d}\bar{L}}{\mathrm{d}t} \tag{18}$$

Thus, the growth rate is simply equal to the rate of change of the first moment with time and does not depend on the shape of the distribution, provided μ_2 and μ_3 are not a function of time.

In most cases, the CSD is not measured throughout the experiment. Usually the only data available are the final crystal size distribution and the desupersaturation profile. Given only this information, the average size $\bar{L}$ can be determined as a function of time by back-calculating the CSD using the desupersaturation profile and the shape of the distribution (i.e. the variance and the skew). Crystal growth rate can then be calculated from the slope of the $\bar{L}$ vs time curve.

Calculation of growth rate

Crystal growth rate is evaluated as follows: at the end of the experiment, time $t = t_f$, the total mass of crystals in the crystallizer is

$$M_f = \rho k_v \int_0^\infty L^3 n \, dL \tag{19}$$

At some earlier time t, all crystals would be ΔL smaller and the crystal mass would be

$$M_t = \rho k_v \int_0^\infty (L - \Delta L)^3 n \, dL. \tag{20}$$

Subtracting Eqn. 20 from Eqn. 19 and substituting Eqns. 10–12 yields an expression for the value of ΔL as:

$$\Delta L^3 - 3\bar{L}\Delta L^2 + 3(\mu_2 + \bar{L}^2)\Delta L + \left(\frac{M_t}{M_f} - 1\right)(\mu_3 + 3\bar{L}\mu_2 + \bar{L}^3) = 0 \tag{21}$$

The cubic equation is then solved for $\Delta L/\bar{L}$ (Appendix I) as:

$$\frac{\Delta L}{\bar{L}} = 1 + (-\alpha + \beta)^{1/3} + (-\alpha - \beta)^{1/3} \tag{22}$$

where

$$\alpha = \frac{1}{2}\left[\frac{M_t}{M_f}\left(1 + 3\frac{\mu_2}{\bar{L}^2}\right) + \left(\frac{M_t}{M_f} - 1\right)\frac{\mu_3}{\bar{L}^3}\right]$$

and

$$\beta = \left[\alpha^2 + \left(\frac{\mu_2}{\bar{L}^2}\right)^3\right]^{1/2}$$

To evaluate the growth rate, the values of $\bar{L}$, μ_2 and μ_3 are calculated from the final crystal size distribution. A small time interval is then chosen and from the concentration profile the value of M_t is found for the beginning of the time interval. Eqn. 22 can then be used to determine the value of ΔL that must have occurred to produce the given change in crystal mass M. Subtraction of ΔL from $\bar{L}$ provides a new value of $\bar{L}$ for the next calculation.

Back-calculation of growth rates can be continued until further calculation shows any crystal size to become less than zero. At this point nucleation is occurring and the values of μ_2 and μ_3 are no longer constant and further calculation with the given method would no longer be valid.

Experimental

Data obtained by Rodriguez-Hornedo (1984) were used for the calculations. Briefly, oxalic acid dihydrate was crystallized from 3 solvent systems, water, 15% (w/w) glycerin : water and 50% (w/w) acetone : water. A saturated solution of oxalic acid dihydrate at 30 °C was cooled at 10 °C/h in a jacketed stirred vessel. When the solution temperature reached 27 °C, three 10/20 mesh seed crystals were added to initiate nucleation. Solution concentration was monitored during the crystallization run by withdrawing fluid samples and measuring the oxalic acid concentration via aliquot titration. The solution supersaturation was calculated knowing the saturation concentration of oxalic acid dihydrate as a function of temperature and solvent.

The crystal size distribution at the end of a run was measured by withdrawing the contents of the crystallizer, filtering, washing and drying the crystals. After weighing, the crystals were sieved and the weight reporting to each sieve fraction noted. The average weight per crystal was determined in each sieve fraction by weighing a known number of crystals from that fraction.

The final CSD was determined by converting the weight percent of crystals on each sieve to number of crystals using the equation:

$$\Delta N_i = \frac{1}{100}\,\frac{M_f w\%_i}{w_i} \qquad (23)$$

where ΔN is the number of crystals on the i^{th} sieve, M_f is the final crystal mass, $w\%_i$ is the weight percent of crystals reporting to the i^{th} sieve and w_i is the average crystal weight on the i^{th} sieve. M_f was determined by the total concentration change during the crystallization run. The first four moments were then calculated from Eqn. 9 using the approximation that $n \approx (\Delta N/\Delta L)$ where ΔL is the change in average crystal size between sieves.

After calculating the moments of the final CSD, Eqn. 22 was used to determine the value of ΔL corresponding to the final growth step. The value of ΔL was then subtracted from each L_i of the final distribution and the resulting values used for the next calculation. This was continued until subtracting the calculated value of ΔL resulted in an L_i value less than zero. A summary of the calculation is given for the aqueous case in Appendix II.

Results and Discussion

The concentration, saturation concentration and temperature profiles of the aqueous run are shown in Fig. 1. The concentration remains constant until the temperature reaches 27° C at which time the seed crystals were added and crystal growth began. During the time period of the growth rate analysis the temperature varied by no more than 2.0° C. The change in temperature does affect the saturated concentration and supersaturation values are calculated using the measured temperature. However, the effect of the temperature variation on the growth rate constant is small and, for this analysis, is assumed to be negligible. A typical supersaturation profile is shown in Fig. 2.

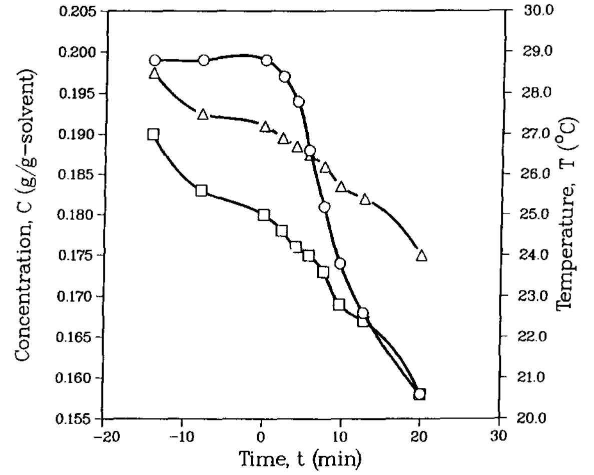

Fig. 1. Concentration (○), saturation concentration (□) and temperature (△) vs time. Solvent: water.

The final CSD and those resulting from the back calculation are shown in Fig. 3. The distributions are parallel and the distance between each line is the value of crystal growth, ΔL, during the corresponding time period, Δt. This is also equal to the change in the mean size, $\Delta \bar{L}$, for the same time period.

Calculated growth rate is plotted vs supersaturation for the 3 solvents in Fig. 4a and vs the normalized supersaturation in Fig. 4b. The

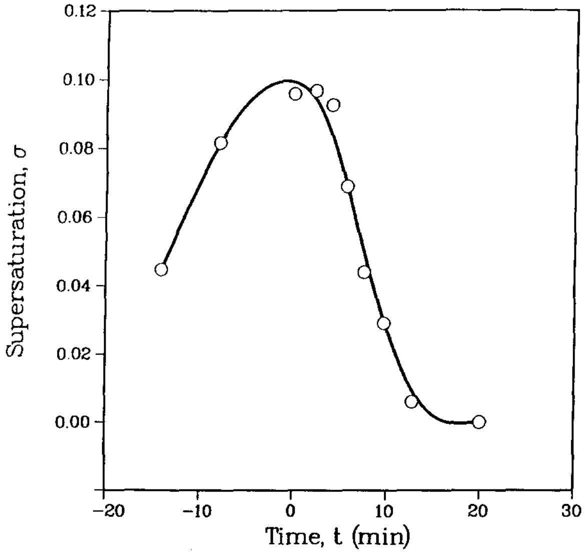

Fig. 2. Supersaturation vs time. Solvent: water.

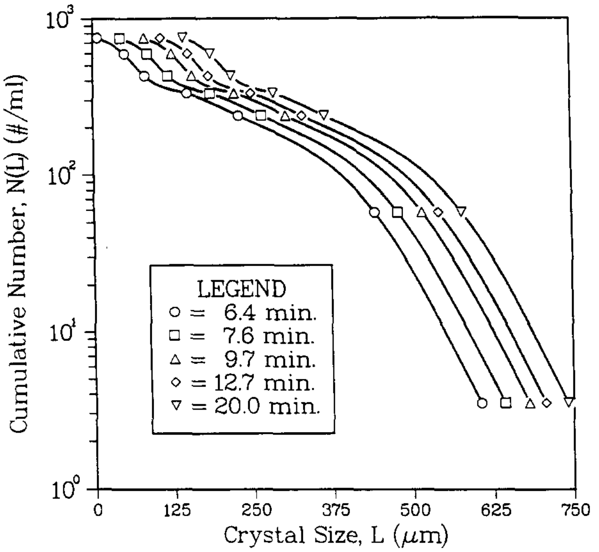

Fig. 3. Cumulative distribution changes due to crystal growth.

values of the growth rate constant, k_g or k'_g, and the growth exponent, a, were found by multiple linear regression of $\ln G$ on $\ln s$ (or $\ln \sigma$) and solvent using the following linear model:

$$\ln G = \beta_0 + \beta_1 \ln s + \beta_2 \text{solvent1} + \beta_3 \text{solvent2} + \epsilon$$

where: solvent1 = 1 for 50% acetone, solvent1 = 0 otherwise; solvent2 = 1 for 15% glycerin, solvent 2 = 0 otherwise.

The beta estimates and their standard errors are given in Table 1. The regression produced an R^2 value of 0.95 using $\ln s$ and 0.94 using $\ln \sigma$. Addition of solvent–ln supersaturation interaction terms did not significantly increase the value of R^2. Thus, the growth exponent, a, which was found to be 1.1 with S.E.M. of 0.081 ($\ln s$) or 0.087 ($\ln \sigma$), is the same for all solvent systems.

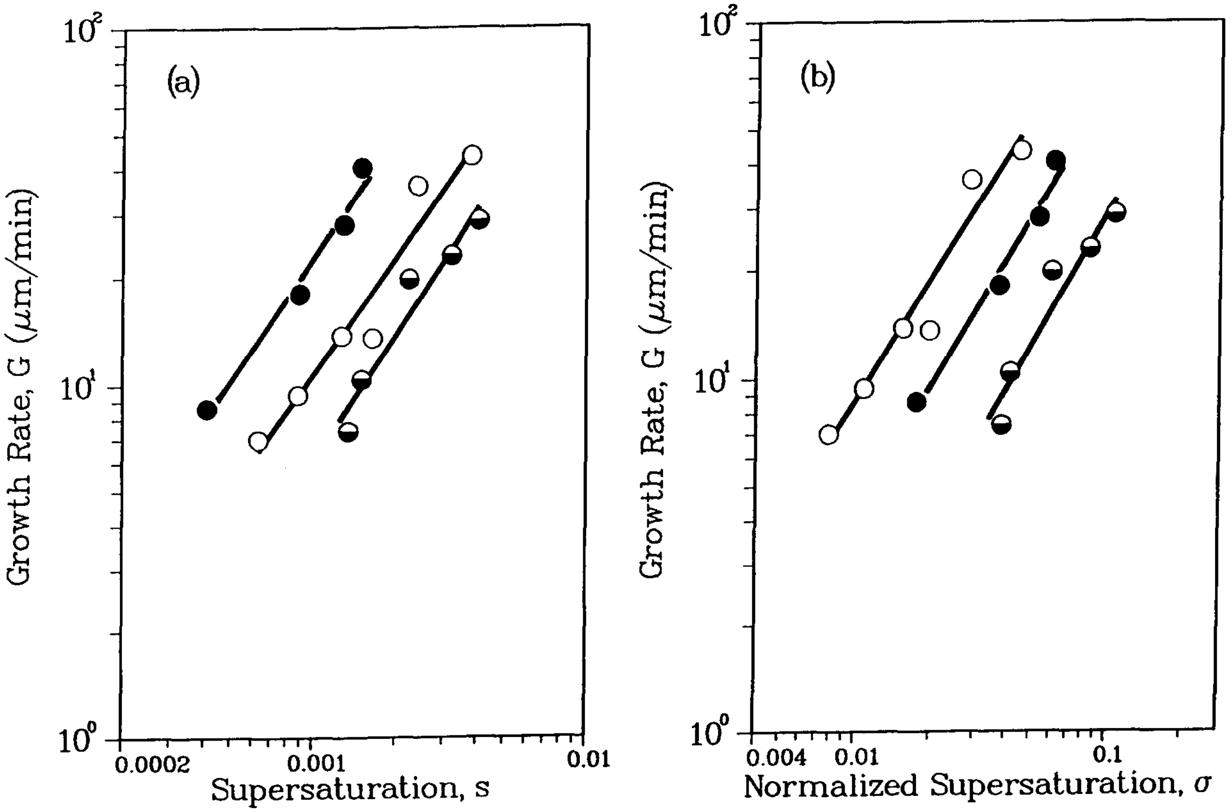

Fig. 4. Growth rate vs supersaturation for three solvents. ●, Water; ◒, 15% glycerine; ○, 50% acetone.

TABLE 1

Estimated values and standard errors of the β coefficients

β_i	Supersaturation			
	$s = x - x_s$		$\sigma = (x - x_s)/x_s$	
	$\hat{\beta}$	S.E.M.	$\hat{\beta}$	S.E.M.
β_0	11	0.57	6.8	0.30
β_1	1.1	0.081	1.1	0.087
β_2	−0.76	0.11	0.64	0.13
β_3	−1.3	0.13	−0.80	0.12

The numerical results of the growth rate constant are given in Table 2.

Note that the relative position of each solvent line is not the same in the two plots. While the slope of all lines is the same, the intercepts, and thus the growth rate constants, depend upon the definition of supersaturation. When the supersaturation, s, is used, the growth rate constant, k_g', is largest in the aqueous system. If the normalized supersaturation, σ, is used, k_g is largest in the 50% acetone system.

This points out the importance of using the normalized supersaturation when making a comparison between different systems. If the supersaturation is not normalized, the growth rate constant will contain information about the solubility of the compound and the growth exponent. (Recall that $k_g = k_g'/x_s^a$.) Thus, differences in growth rate constants could be due to differences in solubility or the growth exponent rather than the growth rate constant.

TABLE 2

Values of the growth rate constant ($\mu m/min$)

Solvent system	Supersaturation	
	$s = x - x_s$	$\sigma = (x - x_s)/x_s$
	k_g'	k_g
Water [a]	4.9×10^4	8.8×10^2
15% Glycerin [b]	1.4×10^4	3.9×10^2
50% Acetone [c]	2.3×10^4	17×10^2

Constants evaluated in the temperature range:
[a] 26.5–25.4°C
[b] 26.0–24.0°C
[c] 27.4–25.8°C.

Conclusions

Desupersaturation profiles can be used in conjunction with the final CSD to calculate crystal growth rates. The method presented does not depend on the shape of the crystal size distribution and can be easily applied to other precipitating systems.

Analysis of the oxalic acid dihydrate system shows that the growth rate is highest in the 50% acetone system and lowest in the 15% glycerine system. The growth exponent is approximately 1 in all solvent systems.

In order to avoid misleading interpretations, it is better to use the normalized supersaturation values defined by σ, since changes in the solubility due to different solvents or different temperatures are accounted for.

Appendix I: detailed derivation of Eqns. 21 and 22

Subtraction of Eqn. 20 from 19 and rearrangement yields:

$$M_t - M_f = -\rho k_v\left(\Delta L^3 m_0 - 3\Delta L^2 m_1 + 3\Delta L m_2\right). \tag{a.1}$$

If both sides are multiplied by $1/M_f$, or $1/\rho k_v m_3$, we obtain:

$$\left(\frac{M_t}{M_f} - 1\right) = -1/m_3\left(\Delta L^3 m_0 - 3\Delta L^2 m_1 + 3\Delta L m_2\right). \tag{a.2}$$

Factoring m_0 from the right-hand side and substituting $\bar{L}$ for m_1/m_0, Eqn. 11 for m_2/m_0 and Eqn. 12 for m_3/m_0 and rearrangement gives:

$$0 = \frac{\Delta L^3}{\bar{L}^3} - 3\frac{\Delta L^2}{\bar{L}^2} + 3\left(\frac{\mu_2}{\bar{L}^2} + 1\right)\frac{\Delta L}{\bar{L}} + \left(\frac{\mu_3}{\bar{L}^3} + 3\frac{\mu_2}{\bar{L}^2} + 1\right)\left(\frac{M_t}{M_f} - 1\right) \tag{a.3}$$

Eqn. a.3 is solved for $\Delta L/\bar{L}$ as follows: a cubic equation of the form $x^3 + bx^2 + cx + d = 0$ can be simplified by the substitution $x = y - b/3$ i.e. $((\Delta L/\bar{L}) = y + 1)$ and becomes:

$$y^3 + py + q = 0 \tag{a.4}$$

where

$$p = 1/3(3c - b^2)$$

and

$$q = \tfrac{1}{27}(27d - 9bc + 2b^3).$$

Equation a.4 has the solution $y = \mathrm{A} + \mathrm{B}$ where

$$A = \left(-q/2 + \sqrt{R}\right)^{1/3} \quad B = \left(-q/2 - \sqrt{R}\right)^{1/3}$$

and

$$R = (p/3)^3 + (q/2)^2.$$

Now, rename $q/2$ as α and $\sqrt{R}$ as β and start substituting:

$$\alpha = q/2 = \frac{1}{2}\left(d - \frac{bc}{3} + \frac{2b^3}{27}\right)$$

$$= \frac{1}{2}\left[\left(\frac{M_t}{M_f} - 1\right)\left(\frac{\mu_3}{\bar{L}^3} + \frac{3\mu_2}{\bar{L}^2} + 1\right)\right.$$

$$\left. + 3\left(\frac{\mu_2}{\bar{L}^2} + 1\right) - 2\right]$$

$$= \frac{1}{2}\left[\left(\frac{M_t}{M_f}\right)\left(\frac{3\mu_2}{\bar{L}^2} + 1\right) + \left(\frac{\mu_3}{\bar{L}^3}\right)\left(\frac{M_t}{M_f} - 1\right)\right] \tag{a.5}$$

$$\beta = \sqrt{R} = \left((p/3)^3 + (q/2)^2\right)^{1/2}$$

$$= \left[\left(\frac{\mu_2^3}{\bar{L}^2}\right)^3 + \alpha^2\right]^{1/2} \tag{a.6}$$

Appendix II: measured crystal size distribution and calculated growth rates of the aqueous system

The CSD measured at the end of the aqueous experiment, the calculated screen sizes and population values are shown in Table 3.

The data from Table 3 can be used with the concentration information in Table 4 to calculate the growth rate corresponding to concentration changes. For example, in the time period from 9.7 min to 12.7 min the concentration change of 0.006 g/g solvent resulted in a 26 μm increase in the

TABLE 3

Final CSD of the aqueous system

Screen	Mesh	L_i † (μm)	$w_i \times 10^5$ g/no.	$w\%_i$	ΔN_i (no./g solvent)	$N(L)_i$ (no./g-solvent)
1	20	744	66.3	5.44	3.5	3.5
2	20/30	581	31.6	40.63	54	58
3	30/40	368	8.02	34.32	180	240
4	40/50	287	3.78	8.43	94	330
5	50/60	221	1.74	4.02	98	430
6	60/80	189	1.08	4.25	160	590
7	80/100	146	0.496	1.85	160	750
8	100/pan	< 146	0.152	1.06	–	–

M_f evaluated as:

M_f = initial conc. minus final conc.

$M_f = 0.199 - 0.157 = 0.042$ g/g-solvent.

† $L_i = (w_i/\rho)^{1/3}$, $\rho = 1.6$ g/cm^3.

TABLE 4

Concentration profile and calculated growth rates for the aqueous system

Time (min)	Δt (min)	C (g/g-solvent)	C_s (g/g-solvent)	M_t (g/g-solvent)	$\bar{L}$ (μm)	$\Delta\bar{L}$ (μm)	G (μm/min)
0		0.199	0.180	0.000			
2.3		0.197	0.178	0.002			
4.1		0.194	0.176	0.005			
5.7		0.188	0.175	0.011			
6.0 *		0.187	0.175	0.012	123		
	0.4					8	20 ‡
6.4 *		0.186	0.175	0.013	132		
	0.2					8	40
6.6 *		0.185	0.174	0.014	140		
	1.0					28	28
7.6		0.181	0.173	0.018	168		
	2.1					38	18
9.7		0.174	0.169	0.025	206		
	3.0					26	8.6
12.7		0.168	0.167	0.031	232		
	7.3					35	4.8 †
20.0		0.158	0.158	0.041	267		
	13.5					3	0.2 †
33.5		0.157	0.157	0.042	270		

* Interpolated values.

† Point not used due to low supersaturation.

‡ Calculation produces size less than zero.

number average size ($\Delta\bar{L}$). This is then equivalent to a growth rate of 8.6 μm/min.

Nomenclature

a	supersaturation exponent
A	crystal surface area (μm^2/g-solvent)
C	concentration (g/g-solvent)
G	crystal growth rate (μm/min)
k_a	area shape factor (1/no.)
k_g	growth rate constant (μm/min)
k_v	volume shape factor (1/no.)
L	crystal size (μm)
$\bar{L}$	average crystal size (μm)
M	crystal mass (g/g-solvent)
m_i	i^{th} moment of the distribution
$n(L)$	population density (no./μm g-solvent)
N_t	total number of crystals (no./g-solvent)
$N(L)$	cumulative number distribution (no./g-solvent)
s	supersaturation, mole fraction difference $(x - x_s)$
t	time (min)
T	temperature (°C)
$w\%_i$	weight % on the i^{th} sieve
w_i	average weight of a crystal on the i^{th} sieve (g/no.)
x	mole fraction of the solute
x_s	mole fraction of the solute at saturation
α	calculated value
β	calculated value
$\hat{\beta}$	estimated beta parameter
β_i	coefficient of linear growth model
ϵ	error term in the linear model
μ_2	variance about the mean
μ_3	skew
ρ	crystal density (g/cm^3)
σ	normalized supersaturation $((x - x_s)/x_s)$

References

De Silva, R.L., Falangas, E. and Creasy, D.E., Crystal growth rate determination from desupersaturation measurements. *Trans. I. Chem. E.*, 58 (1980) 135–137.

Misra, C., and White, E.T., Kinetics of crystallization of aluminum trihydroxide from seeded caustic aluminate solutions. *Chem. Eng. Progr. Symp. Ser.*, 67 (1971) 53–65.

Randolph, A.D. and Larson, M.A., *Theory of Particulate Processes*. Academic, New York, 1971, p. 19.

Rodriguez-Hornedo, N., *Effect of crystallization kinetic parameters on the particle size distribution of oxalic acid dihydrate*, Dissertation, University of Wisconsin-Madison, 1984.

Rodriguez-Hornedo, N. and Carstensen, J.T., Crystallization kinetics of oxalic acid dihydrate: nonisothermal desupersaturation of solutions. *J. Pharm. Sci.* 75 (1986) 552–558.